General Disclaimer

One or more of the Following Statements may affect this Document

- This document has been reproduced from the best copy furnished by the organizational source. It is being released in the interest of making available as much information as possible.

- This document may contain data, which exceeds the sheet parameters. It was furnished in this condition by the organizational source and is the best copy available.

- This document may contain tone-on-tone or color graphs, charts and/or pictures, which have been reproduced in black and white.

- This document is paginated as submitted by the original source.

- Portions of this document are not fully legible due to the historical nature of some of the material. However, it is the best reproduction available from the original submission.

Produced by the NASA Center for Aerospace Information (CASI)

NASA TECHNICAL MEMORANDUM

NASA TM X-73539

NASA TM X-73539

(NASA-TM-X-73539) MODAL DENSITY FUNCTION AND NUMBER OF PROPAGATING MODES IN DUCTS (NASA) 19 p HC A02/MF A01 CSCL 20A

N77-11817

Unclas

G3/71 54572

MODAL DENSITY FUNCTION AND NUMBER OF PROPAGATING MODES IN DUCTS

by E. J. Rice
Lewis Research Center
Cleveland, Ohio 44135

28 29 30 31 1 2 3 4 5 6 7 8 9 10 11 12 13 14 15 16 17 18 19 20 21 22 23 24 25 26 27
NOV 1976
RECEIVED
NASA STI FACILITY
INPUT BRANCH

TECHNICAL PAPER to be presented at the
Ninety-second Meeting of the
Acoustical Society of America
San Diego, California, November 16-19, 1976

E-8699

MODAL DENSITY FUNCTION AND NUMBER OF PROPAGATING MODES IN DUCTS

by E. J. Rice

Lewis Research Center

ABSTRACT

Often raised questions in duct sound propagation studies involve the total number of propagating modes, the number of propagating radial modes for a particular spinning lobe number, and the number of modes possible between two given values of cutoff ratio or eigenvalue. These questions can be answered approximately by using the modal distribution function which is the integral of the modal density function for ducts in a manner similar to that previously published for architectural acoustics. The modal density functions are derived for rectangular and circular ducts with a uniform steady flow. Results from this continuous theory are compared to the actual (discrete) modal distributions.

INTRODUCTION

The question of the number of propagating modes within a small range of mode cut-off ratio has been raised in references 1 and 2. The population density of modes has been shown to be greatest near cut-off and least for the well propagating modes. It has been shown in references 1 and 2 that modes of nearly the same cut-off ratio behave nearly the same in a sound absorbing duct as well as in the way they propagate to the far field outside of the duct. Thus it has been proposed that, rather than handling all of the propagating modes individually, they can be grouped into several cut-off ratio ranges. It is important to know the modal density function to estimate acoustic power distribution in the extension of the above mentioned studies.

STAR category 71

A natural companion of the modal density function is the number of propagating modes possible in a duct. In the more limited case of rotor-stator interaction noise where the mode lobe numbers (m) are restricted (ref. 3) it is of interest to know the number of propagating radial modes for a particular mode lobe number. It is of course possible to enumerate the number of propagating modes by counting them with the use of eigenvalue tables as done in reference 4, but it is much more convenient to have approximate equations for this purpose particularly when large numbers of modes are involved.

Equations for the number and modal density of the propagating modes in circular and rectangular ducts are developed in this paper. The basis for the equations lies in the very analogous problem of normal modes in rooms used in architectural acoustics (refs. 5, 6 are examples).

SYMBOLS

A_{ax}	area of the axial modes in the j, m vector plane, see eq. (27)
A_{OB}	area of the oblique modes in the j, m vector plane, see eq. (29)
c	speed of sound, m/sec
$\mathcal{D}$	modal density function, see eqs. (40) and (42)
D	circular duct diameter, m
F	function of η, ξ, and M, see eq. (26)
F_0	limiting value of F at a particular value of cut-off ratio
f	frequency, Hz
H	rectangular duct height, m
i	$\sqrt{-1}$
j	integer index, see eq. (25)
J_m	Bessel function of first kind of order m

N	total number of modes
N_{ax}	number of modes including $j=0$ and $m=0$ modes only
N_0	number of modes with $m=0$
N_m	number of modes with a particular value of m
N^*	number of modes, sum of N_0 and N^+
N^+	number of spinning modes in one transverse direction
M	uniform steady flow Mach number
m	spinning mode lobe number
m_0	maximum value of m for which first radial mode will propagate
P	acoustic pressure, N/m^2
R	ratio of large to small dimensions in a rectangular duct
r	radial coordinate, m
r_H	hub radius in an annulus, m
r_W	outer wall radius, m
t	time, sec
W	rectangular duct width, m
x	axial coordinate, m
y	transverse coordinate between rectangular duct walls, m
z	transverse coordinate, m
α	eigenvalue
α_0	limiting value of the eigenvalue for which propagation occurs
β	eigenvalue
δ	annulus hub-tip ratio, r_H/r_W
η	frequency parameter, fD/c or fH/c
θ	angular coordinate, radians

ξ mode cut-off ratio, eq. (5) for cylindrical ducts, eq. (24) for thin rectangular ducts

τ propagation coefficient, see eqs. (1), (2), (20), (21), (35)

τ_0 function of m and α_0, see eq. (8)

ω circular frequency, rad/sec

NUMBER OF PROPAGATING MODES

Expressions for the number of propagating modes will be derived in this section. Both circular and rectangular ducts will be considered. These equations will be used in the next section to derive the modal density functions.

Circular Ducts

The expression for the acoustic pressure of a spinning mode in a circular duct is given by

$$P = J_m\left(\frac{\alpha r}{r_W}\right)e^{i\omega t - im\theta - i\frac{\omega}{c}\tau x} \tag{1}$$

where

$$\tau = \frac{-M + \sqrt{1 - (1 - M^2)\left(\frac{\alpha}{\pi\eta}\right)^2}}{1 - M^2} \tag{2}$$

and

$$\eta = \frac{fD}{c} \tag{3}$$

and M is the Mach number of the uniform steady flow in the duct. The condition that the radial particle velocity must vanish at the outer hard wall determines the eigenvalues from

$$J'_m(\alpha) = 0 \tag{4}$$

The problem of modal enumeration amounts to counting the number of solutions to equation (4) such that α is less than some α_0. The quantity α_0 will be interpreted here as the limiting value of the eigenvalue for which sound propagation can occur. This idea of propagation involves the cut-off ratio defined as

$$\xi = \frac{\pi\eta}{\alpha\sqrt{1 - M^2}} \tag{5}$$

When equation (5) is used in equation (2), it is seen that at $\xi = 1$ the radical in equation (2) vanishes and this will be termed cut-off. For $\xi < 1$, the propagation coefficient τ will be complex and damping occurs in the pressure (eq. (1)). Whether a mode is propagating or not depends upon the mode eigenvalue (α) as well as the duct diameter (D), sound frequency (f) and the uniform steady flow Mach number (M). Thus, for the purposes of this development,

$$\alpha_0 = \frac{\pi\eta}{\sqrt{1 - M^2}} \tag{6}$$

The lobe number m_0 is the largest value of m for which the first root of equation (4) is less than α_0.

The properties of the Bessel function eigenvalues will not be considered in detail here. For more detail, reference 5 is suggested and the following eigenvalue properties were obtained from this reference. The properties of the eigenvalues are such that for a given lobe number m, the number of modes with eigenvalue α less than α_0 can be approximated by,

$$N_m(\alpha_0) = \frac{\alpha_0}{\pi}(\sin \tau_0 - \tau_0 \cos \tau_0) + \frac{1}{4} \tag{7}$$

where

$$\cos \tau_0 = \frac{m}{\alpha_0} \tag{8}$$

Equation (7) is very good for large values of α_0 and is fairly adequate even down to α_0 of ten. The total number of modes with α less than α_0 is obtained by summing over equation (7) from $m = 0$ to m_0 (see ref. 5). The result is,

$$N^*(\alpha_0) = \frac{\alpha_0^2}{8} + \frac{1}{2}\left(\frac{1}{2} + \frac{1}{\pi}\right)\alpha_0 \tag{9}$$

(Note; there is an error in reference (5), eq. (15) in the last term). Equation (9) contains the axisymmetric modes ($m = 0$) and the spinning modes in one transverse direction only. The number of axisymmetric modes is (eq. (7), $m = 0$),

$$N_0(\alpha_0) \approx \frac{\alpha_0}{\pi} \tag{10}$$

The number of spinning modes in one transverse direction is thus,

$$N^+(\alpha_0) = N^*(\alpha_0) - N_0(\alpha_0) = \frac{\alpha_0^2}{8} + \frac{1}{2}\left(\frac{1}{2} - \frac{1}{\pi}\right)\alpha_0 \tag{11}$$

Finally the total number of modes in the positive axial direction is

$$N(\alpha_0) = 2N^+(\alpha_0) + N_0(\alpha_0) = \frac{\alpha_0^2}{4} + \frac{\alpha_0}{2} \tag{12}$$

The number of propagating modes is now related to the duct size, steady flow Mach number and sound frequency by using equation (6) to yield,

$$N_0 = \frac{\eta}{\sqrt{1 - M^2}} \tag{13}$$

$$N^+ = \frac{\pi^2\eta^2}{8(1 - M^2)} + \frac{\pi\eta\left(\frac{1}{2} - \frac{1}{\pi}\right)}{2\sqrt{1 - M^2}} \tag{14}$$

and

$$N = \frac{\pi^2\eta^2}{4(1 - M^2)} + \frac{\pi\eta}{2\sqrt{1 - M^2)}} \tag{15}$$

The number of propagating modes is seen to depend only upon the frequency parameter η and the steady flow Mach number M. The number of modes (spinning only, in one direction) have been counted in reference 4 for $M = 0$, $\eta = 30.11$ with a reported result of $N^+ = 1126$. Equation (14) yields $N^+ = 1127$ showing excellent agreement for large values of η. For small values of η and for $M = 0$, figure 1 shows a comparison between an exact mode count and N^* from equation (9) (using eq. (6) with $M = 0$). The agreement is seen to be quite good. Note that the equations do not include the plane wave mode since when $\eta = 0$ then $N = 0$). If this mode were also included (add unity to equations) the agreement between calculated and actual mode counts would be improved at low values of η.

A more general form of equations (13) to (15) can be developed for an arbitrary value of the cut-off ratio rather than just at cut-off ($\xi = 1$). This is done by using equation (5) rather than (6) for α or α_0. The results are,

$$N_0(\xi) = \frac{\eta}{\xi\sqrt{1 - M^2}} \tag{16}$$

$$N^+(\xi) = \frac{\pi^2\eta^2}{8\xi^2(1 - M^2)} + \frac{\pi\eta\left(\frac{1}{2} - \frac{1}{\pi}\right)}{2\xi\sqrt{1 - M^2}} \tag{17}$$

and

$$N(\xi) = \frac{\pi^2\eta^2}{4\xi^2(1 - M^2)} + \frac{\pi\eta}{2\xi\sqrt{1 - M^2}} \tag{18}$$

These give the number of propagating modes with cut-off ratios from infinity to the selected value of ξ. Equations (13) to (15) are thus special cases of equations (16) to (18) with $\xi = 1$.

The number of propagating modes with a particular lobe number (m), frequency parameter (η), and Mach number (M) may be of interest in a circular duct. This number can be calculated directly from equation (7) using equations (8) and (6). An approximation to equation (7) can also be derived by using a series expansion around $m = 0$. The resulting approximation is

$$N_m(m, \eta, M) \approx \frac{\eta}{\sqrt{1 - M^2}} + \frac{1}{4} - \frac{m}{2} + \frac{m^2\sqrt{1 - M^2}}{2\pi^2\eta} \tag{19}$$

Sample calculations using equations (7) and (19) are compared to exact counts in table I for $\eta = 15$ and $M = 0$.

REPRODUCIBILITY OF THE
ORIGINAL PAGE IS POOR

TABLE I. - COMPARISON OF EXACT AND CALCULATED N_m

m	N_m counted	N_m (eq. (7))	N_m (eq. (19))
0	15	15.25	15.25
5	13	12.83	12.83
10	11	10.59	10.59
20	7	6.62	6.60
30	3	3.41	3.29
35	2	2.12	1.89
40	1	1.09	0.65

The agreement using either equation is seen to be quite good. In actual use the calculated N_m would probably be truncated or rounded off to obtain an integer.

Thin Rectangular Duct

The thin rectangular duct is of interest since it approximates an unwrapped thin annular duct (ref. 7) often used in noise suppressors. The boundary condition in the unterminated direction is that the pressure must repeat over a distance of one annulus circumference. The acoustic pressure solution is,

$$P = \cos\left(\frac{2\alpha y}{H}\right) e^{i\omega t - \frac{imz}{r_W} - \frac{i\omega\tau x}{c}} \tag{20}$$

for symmetric modes, with $\sin(2\alpha y/H)$ replacing the cosine for the asymmetric modes. The axial propagation coefficient is

$$\tau = \frac{-M + \sqrt{1 - (1 - M^2)\left\{\left(\frac{\alpha}{\pi\eta}\right)^2 + \left[\frac{m(1 - \delta)}{2\pi\eta}\right]^2\right\}}}{1 - M^2} \tag{21}$$

where now

$$\eta = \frac{fH}{c} \tag{22}$$

and the hub-tip ratio δ is,

$$\delta = \frac{r_H}{r_W} \tag{23}$$

Note that as in the previous section traveling waves in the positive z direction only are included.

The cut-off ratio is defined as,

$$\xi = \frac{\pi\eta}{\sqrt{(1 - M^2)\left\{\alpha^2 + \left[\frac{m(1 - \delta)}{2}\right]^2\right\}}} \tag{24}$$

The hardwall condition at $y = \pm H/2$ requires that

$$\alpha = \frac{j\pi}{2}, \; j = 0, 1, 2, 3, \ldots \tag{25}$$

which includes the eigenvalues for both the sine and cosine functions. Equation (24) can be rearranged (and using equation (25)) to yield,

$$F^2 = \left[\frac{2\eta}{\xi\sqrt{1 - M^2}}\right]^2 = j^2 + \left[\frac{m(1 - \delta)}{\pi}\right]^2 \tag{26}$$

The enumeration of the modes reduces to finding the number of j and m values such that the value of F calculated from equation (26) is less than or equal to a limiting value F_0. This is the same as counting the modes with cut-off ratios greater or equal to a particular value of ξ. Due to the even spacing of the eigenvalues it is easiest to use the vector plane approach of reference 6. Equation (26) may be viewed as a vector equation in the j and m plane and is pictured as such in figure 2. The location of each mode is shown by a dot and has associated with it a unit area of $(1 - \delta)/\pi$. The term axial modes refer to those along both the $j = 0$ and $m = 0$ axes while the oblique modes are all of the remaining modes. The idea is to calculate the area associated with each type of mode and divide this by the unit area to obtain the number of modes. The area associated with the axial modes is

$$A_{ax} = F_0 \left[1 + \frac{(1 - \delta)}{\pi}\right] \tag{27}$$

that part being associated with $m = 0$ being pictured in figure 2. The number of axial modes is thus,

$$N_{ax} = F_0 \left[1 + \frac{\pi}{(1 - \delta)}\right] \tag{28}$$

The area for the oblique modes is

$$A_{OB} = \frac{\pi F_0^2}{4} - \frac{F_0}{2}\left[1 + \frac{(1 - \delta)}{\pi}\right] \tag{29}$$

where half of the area associated with the axial modes has been removed from the quarter circle since this area has already been accounted for with the axial modes. The final result is

$$N^{*}(\xi) = \frac{\pi^2\eta^2}{\xi^2(1 - M^2)(1 - \delta)} + \frac{\eta}{\xi\sqrt{1 - M^2}}\left[1 + \frac{\pi}{(1 - \delta)}\right] \tag{30}$$

which represents the $m = 0$ modes and the transverse modes in one direction only. The number of modes associated with $m = 0$ (use eq. (26)) is,

$$N_0(\xi) = \frac{2\eta}{\xi\sqrt{1 - M^2}} \tag{31}$$

with spinning modes in one direction,

$$N^{+}(\xi) = \frac{\pi^2\eta^2}{\xi^2(1 - M^2)(1 - \delta)} + \frac{\eta}{\xi\sqrt{1 - M^2}}\left[\frac{\pi}{(1 - \delta)} - 1\right] \tag{32}$$

and with the total number of modes being

$$N(\xi) = \frac{2\pi\eta}{\xi\sqrt{1 - M^2}\,(1 - \delta)}\left[\frac{\pi\eta}{\xi\sqrt{1 - M^2}} + 1\right] \tag{33}$$

which represents the $m = 0$ modes and the modes spinning in the plus and minus transverse directions. The number of propagating modes of each type can now be determined by letting the cut-off ratio ξ be unity. Figure 3 shows a comparison of N^{*} (eq. (30)) with an actual count of modes using equation (25). No attempt has been made to reproduce the discrete steps of the actual count (as in fig. 1). The agreement is seen to be quite good and thus the continuous equations can be used to approximate the actual discrete number of modes. Included for comparison is a mode count (using tables of ref. 8) in an annulus with hub-tip ratio (δ) of 2/3. The actual annulus is seen to have somewhat fewer modes than its approximating rectangle but the agreement should improve for higher δ.

The number of modes propagating with a particular lobe number is quite simple to obtain with a thin rectangular duct. Solve for j in equation (26) (with $\xi = 1$) and add unity (to account for the $j = 0$ mode). The result is,

$$N_m(m, \eta, M) = \sqrt{\frac{4\eta^2}{(1 - M^2)} - \left[\frac{m(1 - \delta)}{\pi}\right]^2} + 1 \tag{34}$$

Note that equations (30), (31), and (33) do not contain the plane wave mode. If the plane wave is desired in the count, unity should be added to these equations.

Rectangular Duct

Consider a rectangular duct with smaller dimension H and larger dimension W. The pressure for the symmetric modes is given by

$$P = \cos \frac{2\alpha y}{H} \cos \frac{2\beta z}{W} e^{i\omega t - i\frac{\omega}{c}\tau x} \tag{35}$$

with sine functions used for the asymmetrical modes. A procedure very similar to that in the previous section will yield,

$$N(\xi) = \frac{\pi R \eta^2}{\xi^2(1 - M^2)} + \frac{\eta(R + 1)}{\xi \sqrt{1 - M^2}} \tag{36}$$

with

$$\eta = \frac{fH}{c} \tag{37}$$

and

$$R = \frac{W}{H} \geq 1 \tag{38}$$

Note the frequency parameter is based upon the smaller dimension here. In this case no arguments involving plus or minus direction transverse waves need be made since the cosine or sine function encompass both wave directions. Again with $\xi = 1$ in equation (34) the total number of propagating modes can be estimated.

Note that all of the mode counting equations previously presented consider only the modes propagating in the plux-x direction. If reflections off of an end termination are considered, the number of modes would be doubled.

MODAL DENSITY FUNCTION

The modal density function for all modes in a circular duct will be developed here. Similar procedures can be used for the axisymmetric or the spinning modes or for the other duct shapes if desired.

Differentiation of equation (18) yields

$$\frac{dN(\xi)}{d\xi} = \frac{\pi^2\eta^2}{2\xi^3(1 - M^2)}\left[1 + \frac{\sqrt{1 - M^2}}{\pi\eta}\xi\right] \tag{39}$$

where the sign has been changed such that integration from ξ to ∞ will recover the original mode number equation. When equation (39) is normalized by the total number of propagating modes (eq. (15)) the modal density function is obtained as

$$\mathcal{D} = \frac{1}{N}\frac{dN(\xi)}{d\xi} = \frac{2\left[1 + \frac{\sqrt{1 - M^2}}{\pi\eta}\xi\right]}{\xi^3\left[1 + \frac{2\sqrt{1 - M^2}}{\pi\eta}\right]} \tag{40}$$

The second term in the denominator is usually small for aircraft inlet applications since usually $10 < \eta < 30$. The second term in the numerator can dominate only if

$$\xi > \frac{\pi\eta}{\sqrt{1 - M^2}} \tag{41}$$

which is a very large cut-off ratio (far from cut-off ($\xi = 1$) which is of most interest for acoustic power considerations). The modal density function can thus be well approximated by

$$\mathscr{D} \approx \frac{2}{\xi^3} \tag{42}$$

The same equation can be used for rectangular ducts provided that

$$\xi < \frac{2\pi\eta}{\sqrt{1 - M^2}} \tag{43}$$

for thin rectangular ducts and

$$\xi < \frac{2\pi\eta R}{\sqrt{1 - M^2}\,(R + 1)} \tag{44}$$

for rectangular ducts. Some care should be exercised in using equation (42) for rectangular ducts. In some applications conditions (43) or (44) may not be realized. In aircraft applications where annular ducts are used (rectangular intended to simulate annulus) the frequency parameter (η) is usually around one or two representing a limiting cut-off value beyond the range of interest.

The modal density is seen to be greatest near cut-off ($\xi = 1$) and diminishes rapidly as cut-off ratio is increased. This quantifies the observation of this fact which was stated in reference (1). It is also interesting to note that the modal density function (in its approximate form) depends only upon the cut-off ratio.

CONCLUDING REMARKS

An approximate modal density function has been derived which is valid for both circular and rectangular ducts. This function represents the fraction of the total modal population which is within a small cut-off ratio range. The modal density function was found to depend only upon cut-off ratio. This coincides with the approximate dependence upon cut-off ratio (refs. 1 and 2) of optimum wall impedance, maximum possible sound attenuation, and far field sound radiation. The density function is required to extend an approximate liner design technique based upon the unifying influence of cut-off ratio (ref. 2).

Approximate equations were also presented to estimate the number of propagating modes in circular and rectangular ducts. All of the above are approximate in the sense that continuous equations are presented to represent an inherently discrete phenomenon. The approximation is good provided a sufficiently large number of modes can exist. In cases where only a few modes exist due to low frequency, small ducts, or restricted noise sources (such as some cases of rotor-stator interaction) then the sound propagation should be handled on an individual mode basis.

REFERENCES

1. E. J. Rice, "Acoustic Liner Optimum Impedance for Spinning Modes with Mode Cutoff Ratio as the Design Criterion," Paper No. 76-516 (AIAA, New York, 1976).

2. E. J. Rice, "Inlet Noise Suppressor Design Method Based Upon the Distribution of Acoustic Power with Mode Cutoff Ratio," NASA CP-2001, Nov. 1976.

3. T. G. Sofrin, and J. J., McCann, "Pratt and Whitney Experience in Compressor-Noise Reduction," Preprint 2D2 (Acoust. Soc. Amer., New York, 1966).

4. A. V. Saule, "Modal Structure Inferred from Static Far-Field Noise Directivity," Paper No. 76-574 (AIAA, New York, 1976).

5. G. M. Roe, "Frequency Distribution of Normal Modes," J. Acoust. Soc. Am., 13, 1-7 (1941).

6. P. M. Morse, Vibration and Sound (McGraw-Hill Book Co., Inc., 1948), 2nd ed., p. 390.

7. E. J. Rice, "Spinning Mode Sound Propagation in Ducts with Acoustic Treatment," NASA TN D-7913 (1975).

8. J. W. Converse, and J. D. Hoffman, "Acoustic Standing Waves in a Rocket Combustion Chamber with Ring and Spoke Baffles," Purdue Univ. Tech. Memo 67-5 (1967); also NASA CR-93262.

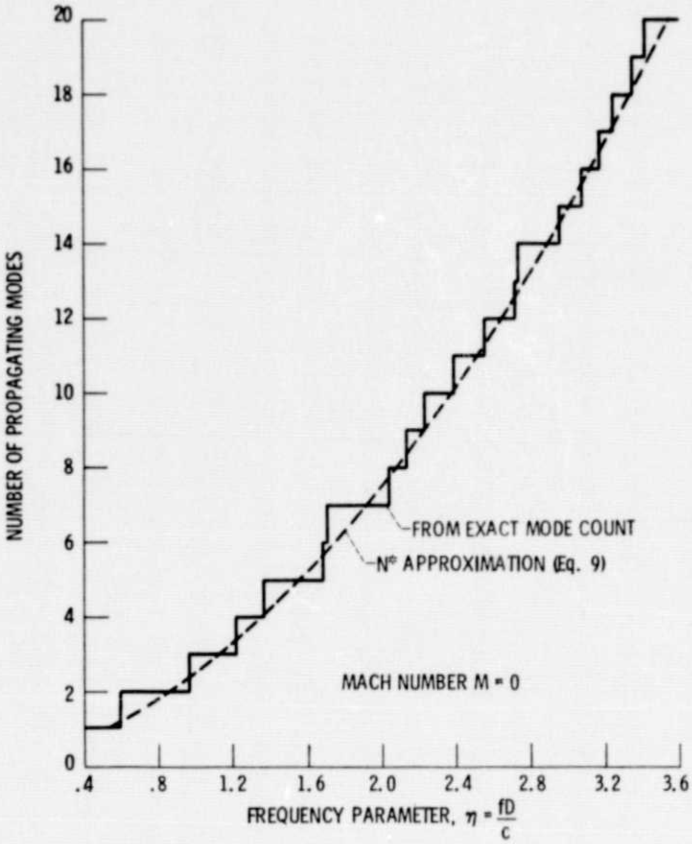

Figure 1. - Comparison of mode count with approximating equation for low values of frequency parameter.

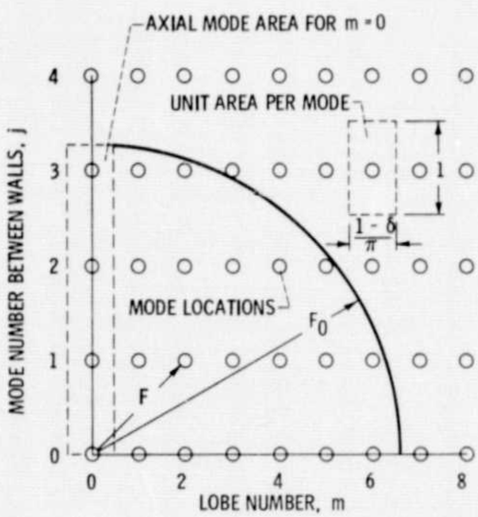

Figure 2. - Vector plane area representation used for mode summation in the thin rectangular duct.

REPRODUCIBILITY OF THE
ORIGINAL PAGE IS POOR

E-8699

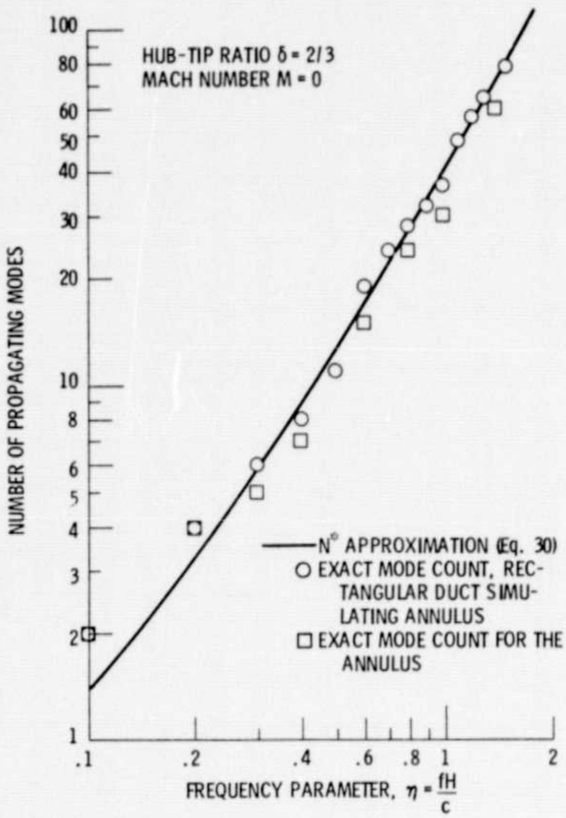

Figure 3. - Comparison of mode counts with approximating equation, rectangular duct simulation of annulus.